Computational studies of pressure distribution of flow through inline dimpled plate.pdf

by

PAPER · OPEN ACCESS

Computational studies of pressure distribution of flow through inline dimpled plate

To cite this article: M Setiawan Sukardin *et al* 2020 *IOP Conf. Ser.: Mater. Sci. Eng.* **885** 012022

IOP Conf. Series: Materials Science and Engineering **885** (2020) 012022 doi:10.1088/1757-899X/885/1/012022

Computational studies of pressure distribution of flow through inline dimpled plate

M Setiawan Sukardin[1,2], Nasaruddin Salam[2], Rustan Tarakka[2], Jalaluddin Haddade[2], and Muhammad Ihsan[3]

[1]Politeknik ATI Makassar, Indonesia
[2]Department of Mechanical Engineering, Hasanuddin University, Gowa, Indonesia
[3]Sekolah Tinggi Teknik Baramuli, Pinrang, Indonesia

Email: setiawan_mkz@yahoo.co.id

Abstract. Dimple plates are widely used for construction and vehicles, especially in car bodies, trains, and aircraft wings. The dimples surface helps to overcome turbulent airflow around vehicles, thereby delaying the separation point and producing fewer vertices and drag. This study aims to predict the pressure distribution occurring over the plate surface with the formation of inline dimple rows on the upper back end. The test is carried out with Computational Fluid Dynamic (CFD) FLUENT program. The test model has a dimension of 300 mm in length, 100 mm in width, and dimples ratio (DR) of 0.5. Dimples are arranged inline as much as 1 to 6 rows. Upstream velocities through dimple plates range from 10 m/s to 20 m/s. The results of the study show that the minimum pressure coefficient occurs at the top front of the plate due to the flow separation that occurs at the front end of the plate. At x/L=0.25 x/L=0.5 and x/L=0.75 (before the dimples formation), a flow pattern returns to normal, this can be seen from the distribution of the relative pressure coefficient that does not change. At the measurement point x/L=0.95 (after dimples formation), there is a decrease in the pressure coefficient. This decrease occurs due to changes in flow characteristics. The pressure coefficient does not change significantly in dimple variations of 2 to 4 rows. Meanwhile, the pressure coefficient decreases with the variation of the 5 and 6-row dimples.

1. Introduction

Recent developments in t vehicle have heightened the need for aerodynamic drag reduction. There have been studies concerning the development of the method for surface friction drag reducti, and the efforts have progressed widely in two ways: methods for delaying the transition of the laminar-turbulent boundary layer and methods for changing or adjusting the structure of turbulent boundary layer [1]. Passive techniques that have been extensiv investigated for turbulent dra reduction include dimples formation on the body surface. The dimpled surface on a golf ball is a well- know application of a non-smooth surface for drag reduction [2]. Several attempts have been made to investigate the reduction in the aerodynamic drag of a vehicle using dimple surface. Wang et al. have conducted numerical studies on generic vehicles to optimize aerodynamic drag using dimple arrays [3]. The dimples surface helps turbulent airflow around the vehicle, thereby delaying the separation point and producing smaller wake and lower form drag. Livya et al. (2015) have evaluated aircraft airfoil drag at 0° - 20° variation angle of attack, which

applies the formation of one dimple [4]. Types of dimples that are applied include square, semi-spherical, compound (a combination of semi-spherical and square) each in the form of concave (inward), and convex (outward). The flow through the dimples forms a small separation bubble. Bubble formation accelerates flow between dimples on the airfoil surface and the boundary layer changes from laminar to turbulent. This transition flow delays the occurrence of flow separation as a cause of decreased drag. Other studies have applied dimple rows on the edge of the back of the Ahmed body with a surface inclination of 25°. The computational approach used is the k-epsilon model on ANSYS Fluent. Dimple ratio variation (DR) were 0.005, 0.2, 0.4 and 0.5 at a speed of 40 m/s where the greatest drag reduction of 1.95% were obtained in the DR 0.4 when compared to the model without dimples [5]. In another study, Zhou et al. (2016) have examined the flow of fluid across the surface of the dimples, with the distribution of surface pressure coefficients measured in a dimple with respective Reynolds numbers; Re=8.2K, Re=36.7K Re=50.5K [6]. Computationally and experimentally, airflow resistance through the dimpled plates has been reviewed in inline and zigzag formations with plates without dimples. The smallest Cd in the inline formation occurs in 2 lines of dimples, while the Cd in the zigzag formation is 1 row of dimples. Decrease in the percentage of the coefficient of resistance between the plates without dimples and the zigzag formation dimpled plates was 5.88%, while the inline formation dimpled plates were 8.65%. [7].

Large-scale asymmetrical vortex structures are formed inside the dimples. The source is located in the front wall of the dimples. Vortex structure tends to intersect the median dimples. In oscillating motion, large-scale asymmetric vortices are periodically released over the back wall at an angle that increases with increasing flow velocity [8]. Dimple, as a passive control, triggers instability that causes significant momentum transport. The shear layer is formed as the flow separation through the first two lines of dimples becomes unstable, and the coherent vortex collection. When vortex develops through plates or dimples, the dynamics of flow become very different due to changes in momentum transport across the boundary layer on staggered arrangement dimples formation 2 and 8 [9].

Fluid flowing on a curved flat plate causes flow separation and boundary layer changes. Separation is caused by the influence of normal force pressure, which is usually called form drag or pressure drag. This study is expected to predict the pressure distribution as a surface drag caused by variations in the number of inline dimple rows on the plate in the quest of an optimal number of dimple rows on objects that have a significant drag form.

2. Method

The test model is in the form of a plate with inline dimple formation. Each model was applied in a variety of dimples rows. Each plate has dimple row, which is applied to the plate top, with a variation of 1 to 6 rows of dimple arrays. The x-axis is in line with the direction of flow velocity U_0. The distance between the center of the dimples on the x-axis and y-axis is 9 mm, respectively. Dimples ratio R/D=0.5. The dimensions of the plate are 300 mm long, 100 mm wide and 25 mm thick. Airflow velocities U_0 through the surface of the dimpled plate very successively 10 m/s, 12 m/s, 16 m/s, 18 m/s, and 20 m/s. The tapping position of the measurement of the pressure distribution in the workpiece model were at x/L=0.1 x/L=0.25 x/L=0.5 x/L=0.75 (before the dimples) and x/L = 0.95 (after the dimples).

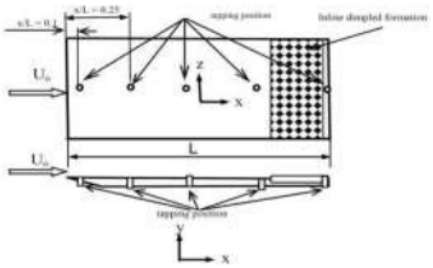

Figure 1. The position of dimples on the plate

Figure 2 illustrates the diameter of the dimples D relative to the distance between the center of the dimple point on the x (Lx) axis and the distance between the center of the dimples on the z-axis (Lz).

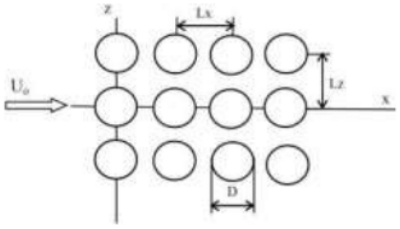

Figure 2. Dimension of inline dimple formation

The computational analysis uses CFD simulation based on ANSYS FLUENT 18.0. The simulation stage starts from drawing the workpiece model using Autodesk Inventor. The meshing process uses ANSYS ICEM CFD 18.0. The assembly of meshing was conducted using tetrahedrons. The number of elements is 1,249,265, and the number of nodes is 227,901. Figure 3 is an example of the result of typical meshing. Figure 4 is a detail of the results of the dimpled plate meshing. The next process is the setup process in ANSYS FLUENT 18.0, simulated in the condition of Re=303K, where air velocity U_0 in a row were 10 m/s, 12 m/s, 14 m/s, 16 m/s, 18 m/s, and 20 m/s on each number of rows dimples. The iteration is attempted to 200 times, followed by the calculation process. Computational results are in the form of pressure distributions at the nodes as measurement points, respectively at x/L=0.1, 0.25, 0.5, 0.75 before the dimples, and 0.95 after the dimples.

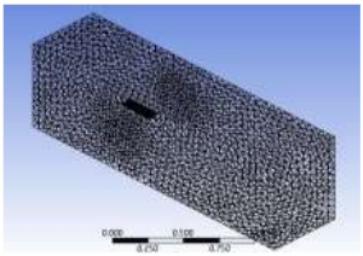

Figure 3. Meshing of test object with 6-row inline dimple formation

Figure 4. Detail of Meshing of the dimpled plate

Pressure drag is the most common form used to define drag on objects. Fluid drag occurs due to the flow, filling the space behind the object, causing a pressure difference between the upstream and downstream flow. Total pressure at the back is lower than that of the front of the object, causing backward suction. The pressure force on flat areas of the plate, which is perpendicular to the flow, causes an enormous drag effect compared to the pressure force on both sides of the flat plate inline to the direction of flow. To acquire the value of this pressure drag force, we need pressure distribution data along the surface of the model. The pressure drag value, a dimensionless parameter, is the coefficient of C_p pressure and commonly expressed as [8].

$$cp = \frac{P - Po}{\frac{1}{2}\rho Uo^2} \qquad (1)$$

p = pressure on the surface of the test model
(Pa) p_o = streamlined pressure or flow line (Pa)
ρ = fluid density
(kg/m^3) U_0 = upstream
speed (m/s)

3. Result and discussion

The present study consists of computational fluid dynamics for variations of the dimple rows on the upper backside of the plate. Upstream velocities range from 10 m/s to 20 m/s. Figures 5 to 9 show that at the measurement point x/L=0.1 (from 10dge of the plate), there is a decrease in pressure in each test model. It shows that the minimum pressure coefficient occurs on the top side of the front plate due to flow separation that occurs at the front end of the plate. At x/L=0.25, x/L=0.5, and x/L=0.75 (before the dimples formation), the flow pattern returns to normal, which can be seen from the distribution of the relative pressure coefficient unchanged.

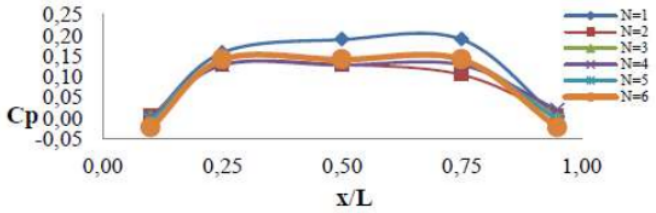

Figure 5. Pressure coefficient for various number of dimple rows of plate with the tapping position, upstream Uo = 10m/s

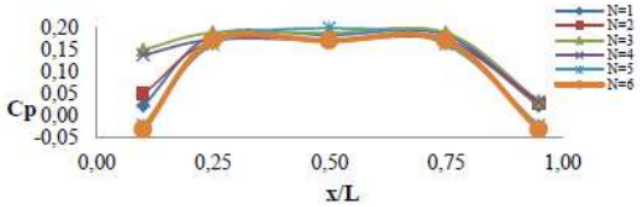

Figure 6. Pressure coefficient for various number of dimples rows of plate with the tapping position, upstream Uo = 12m/s

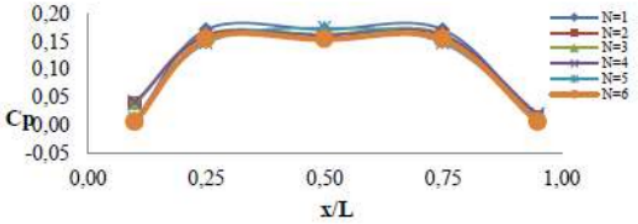

Figure 7. Pressure coefficient for various number of dimples rows of plate with the tapping position, upstream Uo = 14 m/s

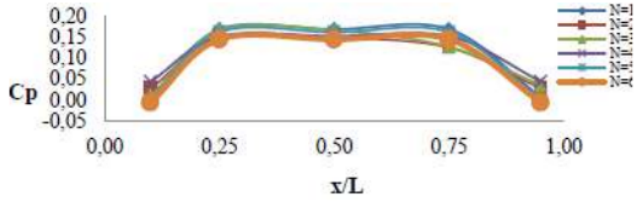

Figure 8. Pressure coefficient for various number of dimples rows of plate with the tapping position, upstream Uo = 16 m/s

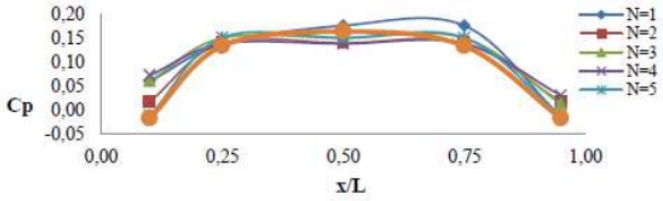

Figure 9. Pressure coefficient for various number of dimples rows of plate with the tapping position, upstream Uo = 18 m/s

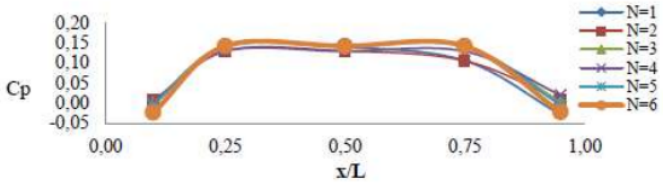

Figure 10. Pressure coefficient for various number of dimples rows of plate with the tapping position, upstream Uo = 20 m/s

Figures 5 to 10 show that at the measurement point x/L=0.1 (from edge of the plate), there is a decrease in pressure in each test model. It shows that the minimum pressure coefficient occurs on the top side of the front side of the plate due to flow separation on the location. At x/L=0.25, x/L=0.5, and x/L=0.75 (before the dimples formation), the flow pattern returns to normal, as indicated by the consistent distribution of the pressure coefficient.

Table 1. Pressure coefficient (C_p) at point after dimple array with x/L=0.95.

Upstream, U_0	Number of dimples rows N					
(m/s)	1	2	3	4	5	6
10	0.001	0.030	0.039	0.032	0.008	0.000
12	0.022	0.025	0.033	0.031	-0.022	-0.032
14	0.009	0.015	0.010	0.020	0.013	0.006
16	0.006	0.027	0.034	0.043	-0.002	-0.007
18	-0.014	0.018	0.013	0.031	-0.012	-0.017
20	-0.029	0.007	0.003	0.020	-0.005	-0.023

From table 1 above, a graph is made of the relationship between the pressure coefficient C_p and the number of dimples N lines in the upstream constant U_0, as in the following figure.

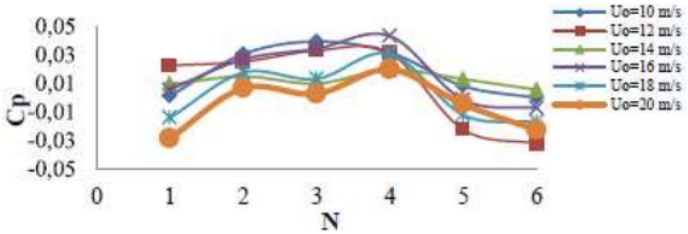

Figure 11. Pressure coefficient at point x/L = 0.95 N number or of rows and different upstream velocity Uo

Figure 11 shows the pressure coefficient at point x/L=0.95 of dimple rows variation at different upstream velocity. The figure also shows that regardless of the variations of the number of rows, no significant change in the pressure coefficient is generated for all upstream speeds. High coefficient of pressure C_p tends to occur in variations of 2 and 4 rows. This shows that the addition of dimple rows up to 4 rows does not contribute to significant friction at the plates. This phenomenon is in line with the smallest coefficient of resistance obtained in 2 rows of dimples [7]. Numbers of rows of 2 to 4 rows can be an alternative to passive flow control, which serves to delay the separation of the surface shape of the objects that change shape drastically, including the shape of the bluff body. Another finding of the research is the development of micro-sized Kelvin-Helmholtz vortex structures over the dimple indentation which confirms the results of Zhou et al. [6]

4. Conclusion

This study concerns to examine numerically the effect of dimple rows in range of upstream velocity from 10 m/s to 20 m/s on the pressure distribution over a flat plate. From the simulation results, the following conclusions can be drawn. The minimum pressure coefficient occurs at the top front of the plate due to the flow separation that occurs at the front end of the plate. At x/L=0.25, x/L=0.5, and x/L=0.75 (before the dimples formation) a flow pattern returns to normal as indicated by the relatively unchanged distribution of the pressure coefficient. At the measurement point x/L=0.95 (after dimples formation), there is a decrease in the pressure coefficient. This decrease occurs due to changes in flow characteristics. Fluid flow through the surface of the dimple causes low-speed recirculating flow, which produces Kelvin-Helmholtz vortex structures. The pressure coefficient does not change significantly in dimple variations of 2 to 4 rows, whereas in dimple variation of 5 and 6 rows, the pressure coefficient decreases.

Acknowledgments

The authors gratefully acknowledge financial support from the Ministry of the Industry Republic of Indonesia under the 2019 F.Y. Grant.

References

[1] Viswanath P R 2002 Aircraft viscous drag reduction using riblets *Prog. Aerosp. Sci.* **38** 571–600
[2] Alam F, Steiner T, Chowdhury H, Moria H, Khan I, Aldawi F and Subic A 2011 A study of golf ball aerodynamic drag *Procedia Eng.* **13** 226–31
[3] Wang Y, Wu C, Tan G and Deng Y 2017 Reduction in the aerodynamic drag around a generic vehicle by using a non-smooth surface *Proc. Inst. Mech. Eng. Part D J. Automob. Eng.* **231** 130–44
[4] Livya E, Anitha G and Valli P 2015 Aerodynamic analysis of dimple effect on aircraft wing *Int. J. Mech. Aerospace, Ind. Mechatron. Manuf. Eng.* **9**
[5] Wong S F and Dol S S 2016 Simulation Study on Vehicle Drag Reduction by Surface Dimples *Int. J. Mech. Mechatronics Eng.* **10** 560–5
[6] Zhou W, Rao Y and Hu H 2016 An experimental investigation on the characteristics of turbulent boundary layer flows over a dimpled surface *J. Fluids Eng.* **138**
[7] Salam N, Tarakka R, Jalaluddin J and Muh S 2018 Fluid Flow Resistance Through Hemispherical Dimpled Plates in Parallel and Zigzag Configurations *Int Rev Mech Eng IREME* **12**
[8] Voskoboinick V A, Turick V N, Voskoboinyk O A, Voskoboinick A V and Tereshchenko I A 2018 Influence of the deep spherical dimple on the pressure field under the turbulent boundary layer *International Conference on Computer Science, Engineering and Education Applications* (Springer) pp 23–32
[9] Beratlis N, Balaras E and Squires K 2014 Effects of dimples on laminar boundary layers *J. Turbul.* **15** 611–27

Computational studies of pressure distribution of flow through inline dimpled plate.pdf

ORIGINALITY REPORT

16%	12%	15%	8%
SIMILARITY INDEX	INTERNET SOURCES	PUBLICATIONS	STUDENT PAPERS

PRIMARY SOURCES

1	Submitted to Universitas Indonesia Student Paper	4%
2	Nasaruddin Salam, Rustan Tarakka, Jalaluddin Jalaluddin, Muh. Setiawan Sukardin. "Fluid Flow Resistance Through Hemispherical Dimpled Plates in Parallel and Zigzag Configurations", International Review of Mechanical Engineering (IREME), 2018 Publication	3%
3	repository.uin-malang.ac.id Internet Source	2%
4	link.springer.com Internet Source	1%
5	P.R Viswanath. "Aircraft viscous drag reduction using riblets", Progress in Aerospace Sciences, 2002 Publication	1%
6	journals.sagepub.com Internet Source	1%

7	doc-pak.undip.ac.id Internet Source	1 %
8	tubdok.tub.tuhh.de Internet Source	1 %
9	Submitted to Universiti Teknologi MARA Student Paper	1 %
10	Syahrir Habiba, Nasaruddin Salam, Rustan Tarakka, Jalaluddin, Muhammad Ihsan. "Distribution of fluid flow pressure through tandem square cylinders with the addition of triangular cylinder as a disturbance object", IOP Conference Series: Earth and Environmental Science, 2021 Publication	<1 %
11	eprints.utm.my Internet Source	<1 %
12	Zhou, Wenwu, Yu Rao, and Hui Hu. "An Experimental Investigation on the Characteristics of Turbulent Boundary Layer Flows over a Dimpled Surface", Journal of Fluids Engineering, 2015. Publication	<1 %
13	researchbank.rmit.edu.au Internet Source	<1 %
14	asu.pure.elsevier.com Internet Source	<1 %

15	vuir.vu.edu.au Internet Source	<1%
16	Yiping Wang, Cheng Wu, Gangfeng Tan, Yadong Deng. "Reduction in the aerodynamic drag around a generic vehicle by using a non-smooth surface", Proceedings of the Institution of Mechanical Engineers, Part D: Journal of Automobile Engineering, 2016 Publication	<1%

Exclude quotes	On	Exclude matches	< 5 words
Exclude bibliography	On		